

https://dspace.org/

DETECTING ASH MIDDENS USING REMOTE SENSING TECHNIQUES: THE CASE OF SOUTHERN GAUTENG, SOUTH AFRICA

Siteleki, Mncedisi

2022-12
South African Archaeological Bulletin
https://hdl.handle.net/10539/40205

Downloaded from a DSpace repository. https://dspace.org/

South African Archaeological Society

DETECTING ASH MIDDENS USING REMOTE SENSING TECHNIQUES

Author(s): MNCEDISI SITELEKI

Source: *The South African Archaeological Bulletin* , December 2022, Vol. 77, No. 217 (December 2022), pp. 163-171

Published by: South African Archaeological Society

Stable URL: https://www.jstor.org/stable/10.2307/27200586

JSTOR is a not-for-profit service that helps scholars, researchers, and students discover, use, and build upon a wide range of content in a trusted digital archive. We use information technology and tools to increase productivity and facilitate new forms of scholarship. For more information about JSTOR, please contact support@jstor.org.

Your use of the JSTOR archive indicates your acceptance of the Terms & Conditions of Use, available at https://about.jstor.org/terms



South African Archaeological Society is collaborating with JSTOR to digitize, preserve and extend access to *The South African Archaeological Bulletin*

This content downloaded from 41.216.201.199 on Sat, 13 Jan 2024 10:54:34 +00:00
All use subject to https://about.jstor.org/terms

Field and Technical Report

DETECTING ASH MIDDENS USING REMOTE SENSING TECHNIQUES: THE CASE OF SOUTHERN GAUTENG, SOUTH AFRICA

MNCEDISI SITELEKI

School of Architecture & Planning, University of the Witwatersrand, WITS, 2050, Johannesburg, South Africa
(Email: mncedisi.siteleki@wits.ac.za)

(Received May 2022. Revised September 2022)

ABSTRACT

South Africa is home to thousands of architectural remnants such as stone-walled structures and ash middens from the Late Iron Age (AD 1300–1800). Ash middens reflect the political and economic lifeways of Iron Age communities. However, the process of identifying and mapping ash middens with traditional survey techniques can be time-consuming and difficult due to dense vegetation. This report aims to assess the performance of two supervised classification techniques, Maximum Likelihood Classification (MLC) and Support Vector Machine (SVM), in detecting ash middens on two multispectral satellite images – GeoEye1 and SPOT5 – in Gauteng, South Africa. The objective is to also assess the ability of the sensors in capturing the spectral signatures of the ash middens. The high reflectance of ash middens relative to other land-cover classes indicates that they have distinct spectral signatures. GeoEye1 is better than SPOT5 in the detection of ash middens because its high spectral and spatial resolution allows for more detailed and accurate mapping. SVM, although advanced, is not a significantly better classification technique for detecting ash middens compared to MLC. This report presents a promising avenue for detecting archaeological ash middens in this part of the world using remote sensing techniques.

Keywords: ash middens, classification, GeoEye1, SPOT5, stone-walled structures.

INTRODUCTION

South Africa is home to thousands of stone-walled structures (SWS) and ash middens from the Late Iron Age (AD 1300–1800). Ash middens are piles of rubbish or ash heaps (Renfrew & Bahn 1991; Boeyens & Hall 2009; Boeyens & Plug 2011). Remnants of ash middens provide a profound reflection on the political and economic lifeways of Iron Age communities. According to Boeyens and Plug (2011), the larger the midden, the richer and more powerful was the ruling community, or court that produced it. Therefore, locating middens and studying their position within the overall configuration of surrounding settlements is crucial for understanding associated power relations. The process of identifying and mapping ash middens with traditional survey techniques can be time-consuming and difficult due to dense vegetation. Multispectral satellite imagery classification offers the potential to speed up this process.

This report detects and compares ash middens on different multispectral satellite images – GeoEye1 and SPOT5, in this case. In the process, it evaluates the multispectral sensors' ability to detect the spectral signatures of ash middens. Two interrelated questions drive this study: 1) Do ash middens have a distinctive spectral signature that allows for their automatic detection on multispectral satellite images? 2) How does the accuracy of automated classification of ash middens compare on different multispectral satellite image resolutions? The aim is to assess the performance of two supervised classification techniques, Maximum Likelihood Classification (MLC) and Support Vector Machine (SVM) in detecting ash middens on GeoEye1 and SPOT5. Using multispectral imagery at high (GeoEye1) and medium (SPOT5) resolution offers a new approach to analysing archaeological features. Accurately classifying ash middens on the selected images can potentially lead to less time and money spent in the field, thereby reducing the labour intensiveness of archaeological fieldwork.

The introduction of remote sensing and the enhancement of satellite imagery has had profound advantages in archaeology for settlement discovery and distribution (Parcak 2009; MacQuilkan & Sadr 2010; Sadr 2012; Abrams & Comer 2013; Keay *et al*. 2014). These include: i) its speed, which reduces costs, time and the potential risk associated with archaeological survey and excavations; ii) the establishment of site strategies pertaining to conservation and preservation (Lasaponara & Masini 2011). In southern African archaeology, the use of remote sensing reveals the extent and diversity of SWS, and it would have been impossible to get such good results from ground survey (Seddon 1968; Maggs 1976; Taylor 1979; Mason 1986; Sadr & Rodier 2012; Hunt & Sadr 2014).

STUDY AREA

The SWS and surrounding ash middens are found in the southern Gauteng region of South Africa, within what is now known as the Suikerbosrand nature reserve. The analysis was conducted on a 49 ha area (Fig. 1) that extends a little over Suikerbosrand to an adjacent farm, which was selected particularly for its richness of ash middens and SWS. Suikerbosrand lies between the Vaal River and the city of Johannesburg and is predominantly covered by hills and valleys that extend over 80 km^2 (Mason 1986; Sadr & Rodier 2012).

METHODS AND MATERIALS

DATA COLLECTION

The satellite images were acquired during winter: June 2013 (GeoEye1) and August 2013 (SPOT5), and their properties are presented in Tables 1 and 2. Ground truthing was done during late spring of 2015 using a handheld GPS device. During this latter period, 39 known ash middens and SWS were recorded in the study area. Several coordinates were recorded from the centre to the edge of each ash midden at 1 m intervals.

IMAGE PRE-PROCESSING

Pre-processing an image prevents atmospheric interference from compromising the quality of the results when performing analyses on satellite imagery, thus significantly increasing the reliability of inspection. Hence images must be radiometrically

This content downloaded from
41.216.201.199 on Sat, 13 Jan 2024 10:54:34 +00:00
All use subject to https://about.jstor.org/terms

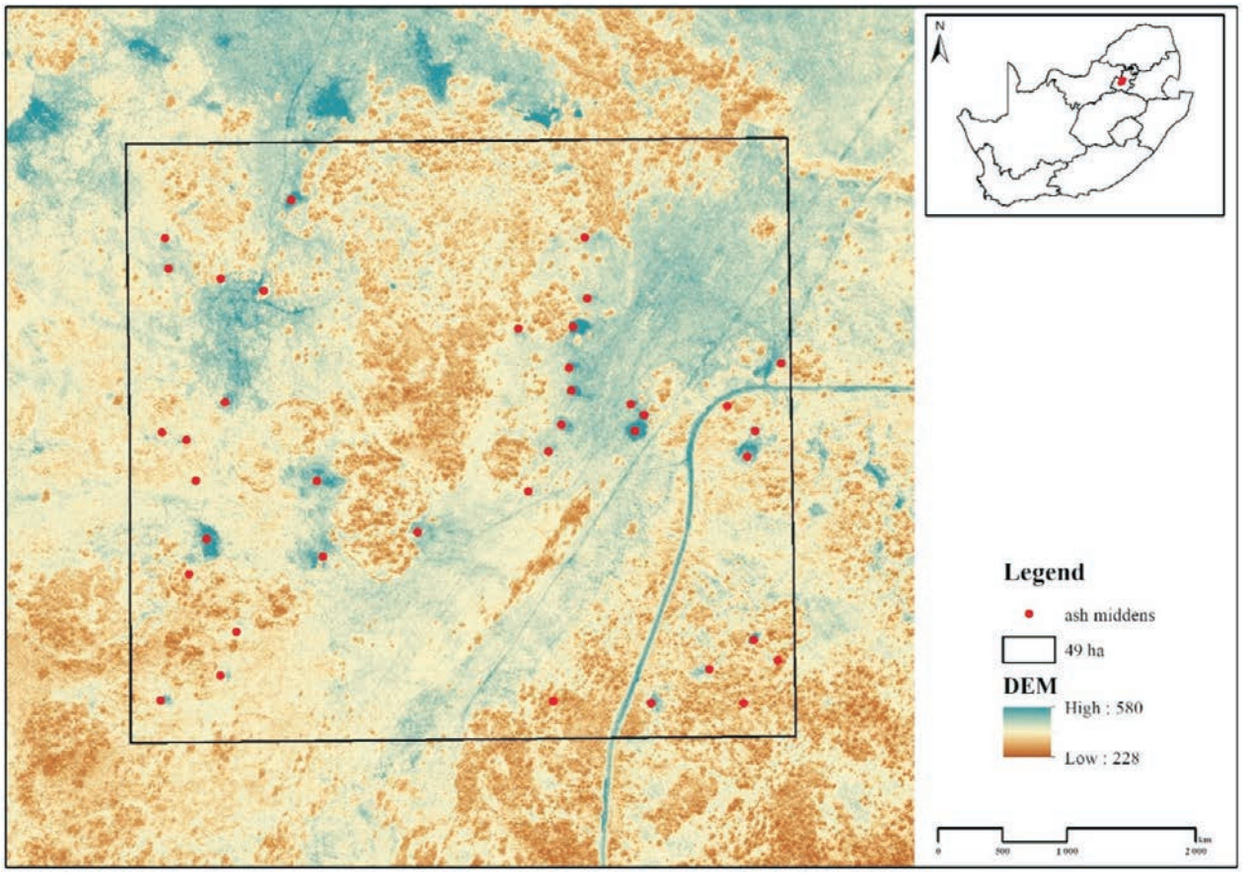


FIG. 1. *Study area in southern Gauteng, South Africa.*

TABLE 1. *SPOT5 properties (adapted from www.spotimage.com).*

Mode	Spatial resolution (m)	Spectral resolution (nm)
PANCHROMATIC	2.5–5	480–710
MULTISPECTRAL	10	500–590 (green)
	10	610–680 (red)
	10	780–890 (near-infrared)
	20	1.580–1.750 (mid-infrared)

TABLE 2. *GeoEye1 properties (adapted from www.digitalglobe.com). GDS: ground sampling distance.*

Mode	Spatial resolution (cm)	Spectral resolution (nm)
PANCHROMATIC	41 GSD at Nadir	450–800 (black and white)
MULTISPECTRAL	1.65 GSD at Nadir	450–510 (blue)
	1.65 GSD at Nadir	510–580 (green)
	1.65 GSD at Nadir	655–690 (red)
	1.65 GSD at Nadir	780–920 (near-infrared)

and spectrally calibrated before analysis (Tehrany *et al*. 2014). Calibration compensates for radiometric errors from sensor defects, variations in scan angle, and system noise, to produce an image that represents true spectral radiance at the sensor (ENVI 2006; Adelabu *et al*. 2014). Pre-processing was conducted with FLAASH, a technique that corrects wavelengths in the visible through near-infrared and shortwave infrared regions (ENVI 2006; Adelabu *et al*. 2014). With its ability to support multispectral sensors, FLAASH is better suited for pre-processing GeoEye1 and SPOT5.

TABLE 3. *Land-cover classes; stone-walled structures (SWS). Sparsely vegetated areas (333) under Class 3: Forests and semi-natural areas. Discontinuous urban fabric (112) under Class 1: Artificial areas. See Bossard* et al. *(2000: 22) for the rest of the classes.*

Land-cover class	Description
Ash middens (112)	Ash heap especially around SWS
Soil (333)	Surface with no vegetation
Scattered vegetation (333)	Mixed vegetation scattered across the landscape
Archaeological features (112)	SWS
Road (112)	Built-up area

DATA ANALYSIS

GeoEye1 and SPOT5 were processed on ENVI 5.2 software to classify (based on training and test samples) the study area. Five land-cover classes (considering the CORINE technical guide) were selected because the study area does not comprise a highly differentiated landscape (Table 3). The landscape consists mainly of open dry land and vegetation. There are no surrounding features such as rivers that can be included in the classes. This study draws from research that has shown that ash middens can be identifiable on satellite imagery (Sadr & Rodier 2012) and black and white aerial photographs (Denbow 1979) with the naked eye as light-coloured patches, especially around SWS. Ash middens (and SWS) that were identified on the satellite images were compared to those identified from the ground truthing.

CLASSIFICATION AND BANDS

Land-cover classification can be supervised or unsupervised. In a supervised classification, the researcher selects training sites (areas representing a unique land-cover type) on a given satellite image in order to identify classes (Sisodia *et al*.

This content downloaded from
41.216.201.199 on Sat, 13 Jan 2024 10:54:34 +00:00
All use subject to https://about.jstor.org/terms

2014). In an unsupervised classification, on the other hand, the researcher's knowledge of identifying classes for the classification is not required because spectral clusters run automated classifications (Sisodia *et al*. 2014). Supervised classification was employed because it gives better accuracy when, for instance, a satellite image has the same reflectance for multiple classes (Erener 2013; Sisodia *et al*. 2014: 1418).

Supervised classification techniques, MLC and SVM, were employed. MLC is regarded as one of the most used and effective classifiers that produces accurate results (Foody & Mathur 2006: 181; Otukei & Blaschke 2010; Aguirre-Gutierrez *et al*. 2012; Erener 2013; Sisodia *et al*. 2014). MLC is a pixel-based parametric classification technique that estimates a statistical probability based on the inputs of classes created from training sites whereby a pixel is ascribed to the class (i.e. respective land-cover class) it most likely belongs to (Otukei & Blaschke 2010; Aguirre-Gutierrez *et al*. 2012; Mondal *et al*. 2012; Sisodia *et al*. 2014).

SVM is a pattern classification method that hosts a distribution-free algorithm with the potential of overcoming poor statistical estimation (Li *et al*. 2012; Tehrany *et al*. 2014). It obtains better empirical accuracy and more generalisation capabilities; especially when working with small training sample sizes (Mountrakis *et al*. 2011; Li *et al*. 2012). The different characteristics of MLC and SVM make them ideal for comparison.

Supervised classification techniques use training sites that are digitised for each land-cover class. A stratified random sample technique was used to digitise the sites because it allows for the selection of a random sample within each land-cover class. The sample of training sites varied due to the images' different spatial resolutions. Between 50–70 training sites were digitised on GeoEye1, and 30–50 on SPOT5. GeoEye1 has a higher spatial resolution (1.65 cm) where one can zoom into more pixels and digitise more training sites, while SPOT5's lower spatial resolution (10 m) means one is able to digitise fewer training sites. SVM and MLC classifications were conducted on the 49 ha area and then tested on a wider region covered by GeoEye1 and SPOT5 around the study area. When conducting classifications, two band comparisons were made on GeoEye1 and SPOT5. Band Combination 1 (BC1) has the same bands and Band Combination 2 (BC2) has different bands. GeoEye1 and SPOT5 have three identical bands and different fourth bands (Tables 1 and 2).

The first comparison, BC1:

- GeoEye1: green, red, near-infrared.
- SPOT5: green, red, near-infrared.

The second comparison, BC2:

- GeoEye1: red, green, blue.
- SPOT5: red, green, mid-infrared.

Comparing BC1 on GeoEye1 and SPOT5 was done to assess the performance of the identical bands in identifying middens. Comparing BC2 was done to assess the impact of the blue and mid-infrared bands on GeoEye1 and SPOT5, respectively.

The measurement of reflected or emitted radiation from surface features is important because such features reflect or absorb the sun's radiation differently. The level of reflectance and absorption depends on the physical and chemical attributes of the surface features in question, like moisture and surface roughness (Erener 2013; Sisodia *et al*. 2014). Variations in reflectance and absorption allow for the identification of various surface features by examining their spectral reflectance patterns and arbitrary profiles. For instance, the reflectance of green vegetation tends to be high in the near-infrared band (Erener 2013). Reflectance on soil is influenced by soil texture and surface roughness. Vegetation has higher reflectance in the near-infrared band than soil.

BC1 and BC2 were compared using an arbitrary profile that refers to the pixels of any image that sit beneath a transect (Adelabu *et al*. 2014; www.harrisgeospatial.com). This was done by drawing an arbitrary profile line across an area that had a variety of classes (i.e. vegetation, ash middens, SWS, soil) on the study area to examine the pixels of each image when using BC1 and BC2 (Figs 2–3). The profile was drawn on the same area across BC1 and BC2 on GeoEye1 and SPOT5.

ACCURACY ASSESSMENT

The most common approach for assessing classification accuracy is to compare the classified land-cover type with the spatial and temporal data with which it corresponds (Comber *et al*. 2012; Comber 2013). This method is known as the confusion matrix. The confusion matrix considers the overall accuracy, producer and user accuracies, which give statistical measures of the precision and reliability of the classified information and the extent to which they are correct or incorrect (Comber 2013; Rimal *et al*. 2019).

The kappa coefficient values further coincided with the accuracy assessment results. The kappa (κ) coefficient measures the agreement between the classification and generated pixels that have been ground-truthed for accuracy (i.e. ground-truthed pixels) (Comber *et al*. 2012). A kappa value of 1 represents a perfect agreement, whereas 0 signifies no agreement. In order to better articulate the reliability of the overall accuracy and the kappa coefficient, the user and producer accuracies were calculated. User accuracy refers to the chance that a pixel assigned as a particular land-cover class (refer to Table 3) on the image is that particular class (Adelabu *et al*. 2014; Rimal *et al*. 2019). Producer accuracy refers to the chance that a particular land-cover class representing an area on the ground is classified as that class (Adelabu *et al*. 2014; Rimal *et al*. 2019). Both user and producer accuracies are estimated from the results of the accuracy assessment.

However, there are limitations to utilising the confusion matrix in that it does not give information pertaining to the spatial spread of the error level (Comber *et al*. 2012; Comber 2013). Furthermore, the overall accuracy provided by the confusion matrix may not be suitable for sub-regions within the land-cover classes where, in reality, the accuracy levels may be higher or lower than the overall one (Comber *et al*. 2012; Comber 2013). The confusion matrix was conducted for MLC and SVM on GeoEye1 and SPOT5 using regions of interest. Regions of interest simply refer to the geographical coordinates obtained using a GPS and from digitising.

RESULTS

CLASSIFICATION

After running the supervised classifications, the results were visualised on maps. Figures 4–7 show BC1 and BC2 for SPOT5 and GeoEye1 classified using MLC and SVM, respectively. One can immediately identify differences in the selected band combinations between GeoEye1 and SPOT5. GeoEye1 maps show greater detail with respect to the land-cover classes as opposed to SPOT5. In all the maps, a black outline has been drawn to delineate known ash middens used as test middens within the study area. Similarly, a grey outline has been used to delineate SWS.

It is clear from Figures 4–7 that the black outline sits atop the bright green colour representing ash middens on GeoEye1 more than on SPOT5. For example, 15 out of 39 black outlines sit

This content downloaded from
41.216.201.199 on Sat, 13 Jan 2024 10:54:34 +00:00
All use subject to https://about.jstor.org/terms

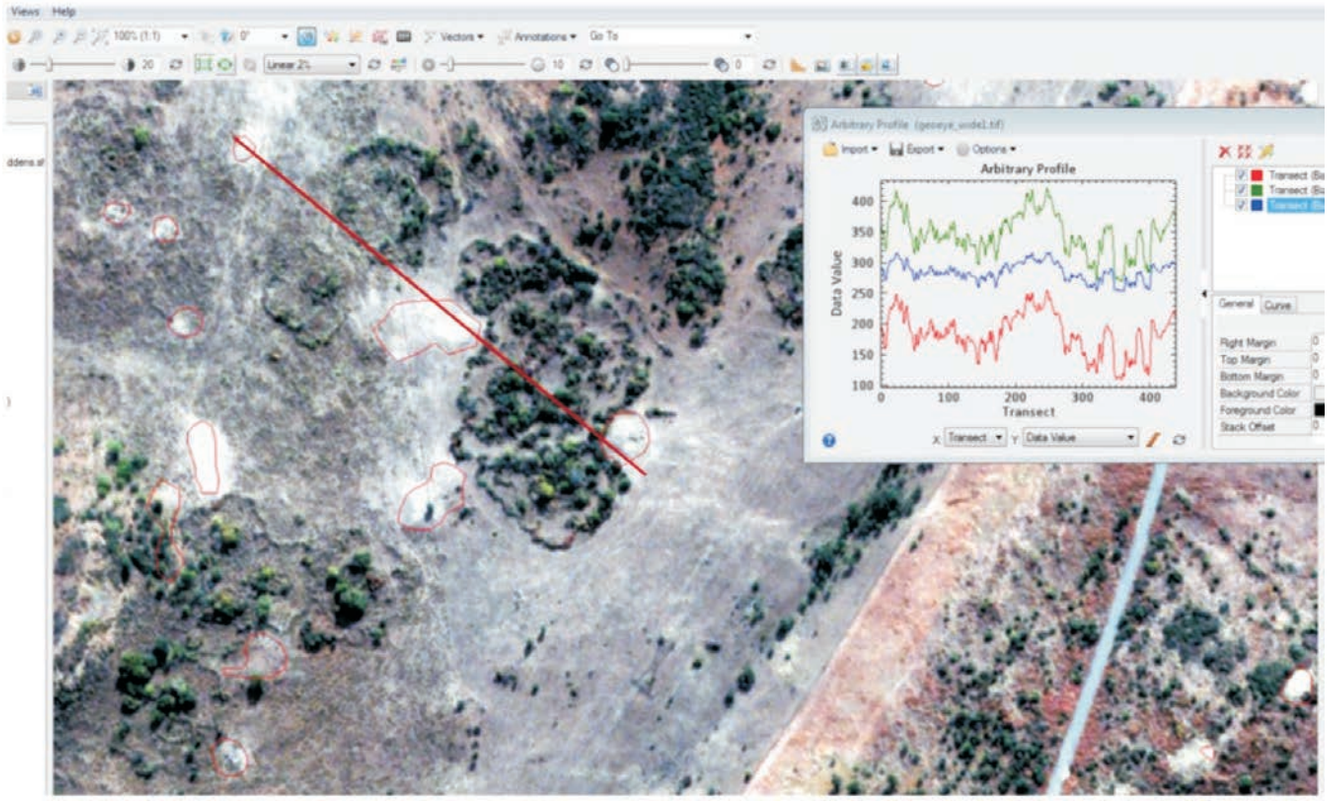


FIG. 2. *An example of an arbitrary line (red) drawn across ash middens on the image (GeoEye1).*

on classified ash middens on SPOT5 produced with MLC on BC1. Conversely, over 25 black outlines sit on classified ash middens on GeoEye1 classified using MLC on BC2. On the other hand, the grey outline is less often identified on the pink colour representing SWS. This signifies that ash middens are more accurately classified compared to SWS. Considering the lack of variety (few land-cover classes) on the study area landscape, it is fairly reasonable to suggest that other land-cover features (e.g. road, soil) were well classified.

ACCURACY ASSESSMENT AND KAPPA COEFFICIENT

The classification accuracy of MLC and SVM was evaluated using the confusion matrix. Figures 8–9 show that the classification techniques achieved higher overall accuracy on GeoEye1 as opposed to SPOT5. With BC1, higher accuracy (97%) was achieved when applying MLC and SVM on GeoEye1. On SPOT5, MLC and SVM were lower at 57%. Applying MLC and SVM on BC2 provided somewhat different results as illustrated in Figures 8–9. MLC and SVM produced higher accuracy on

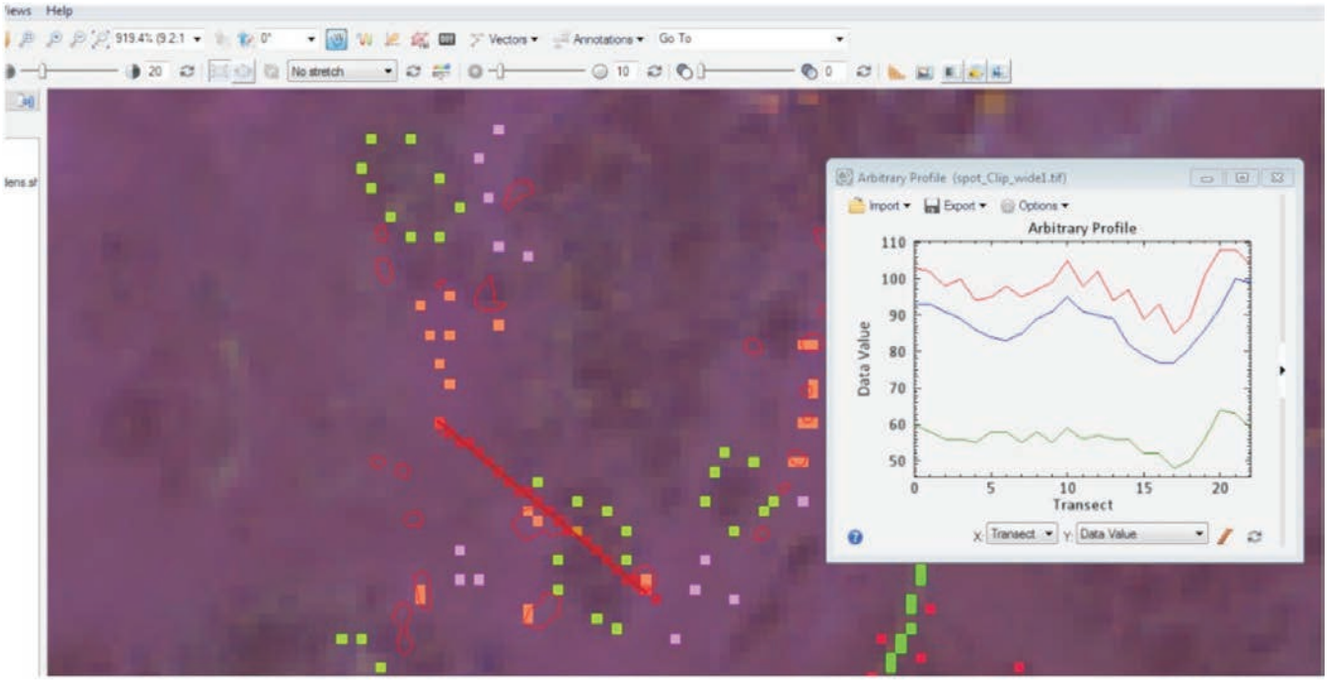


FIG. 3. *An example of an arbitrary line (red) drawn on SPOT5.*

This content downloaded from
41.216.201.199 on Sat, 13 Jan 2024 10:54:34 +00:00
All use subject to https://about.jstor.org/terms

GeoEye1 (although not as high as when using BC1). MLC and SVM yielded lower accuracy on SPOT5 compared to GeoEye1. Consequently, adding mid-infrared to green and red bands on SPOT5 increased MLC and SVM accuracy results contrary to when using BC1.

Overall, there is a perfect relationship between the classification and ground-truthed pixels on GeoEye1 when using BC1 or BC2. The situation is different for SPOT5. There is a relatively poor relationship when using BC1, but a perfect relationship when using BC2, i.e. replacing near-infrared with mid-infrared.

USER AND PRODUCER ACCURACY

In estimating these accuracies, the total number of classi-

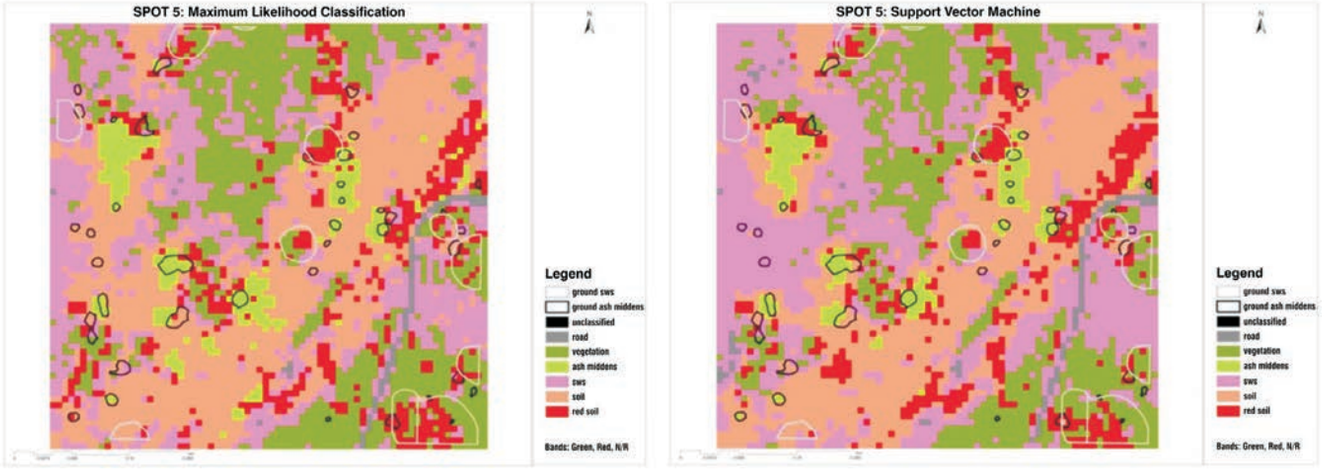


FIG. 4. (**Left**) *BC1 for SPOT5 classified using MLC.* (**Right**) *BC1 for SPOT5 classified using SVM.*

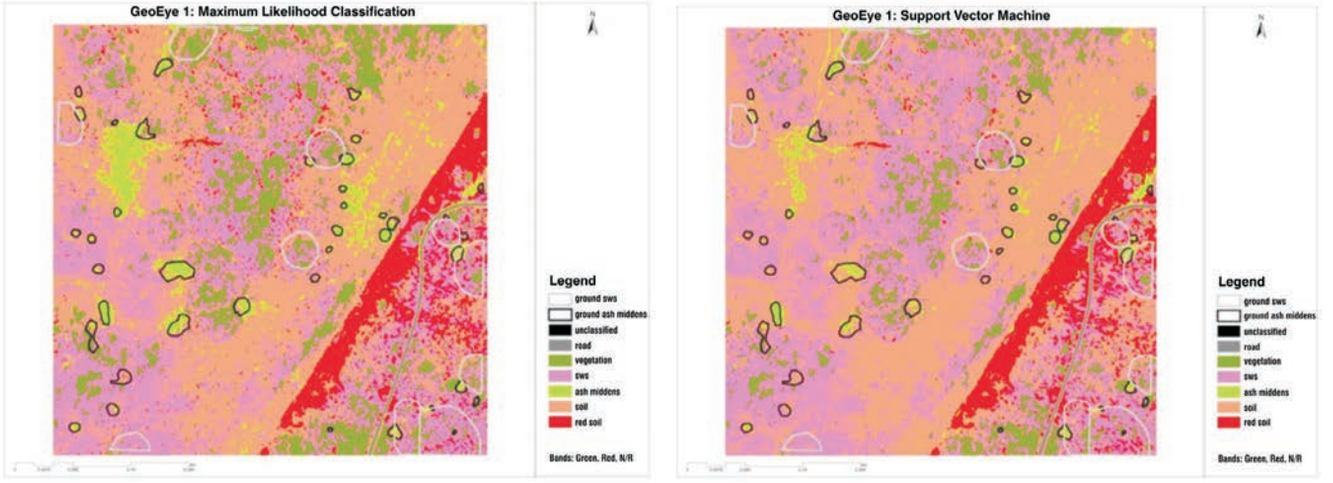


FIG. 5. (**Left**) *BC1 for GeoEye1 classified using MLC.* (**Right**) *BC1 for GeoEye1 classified using SVM.*

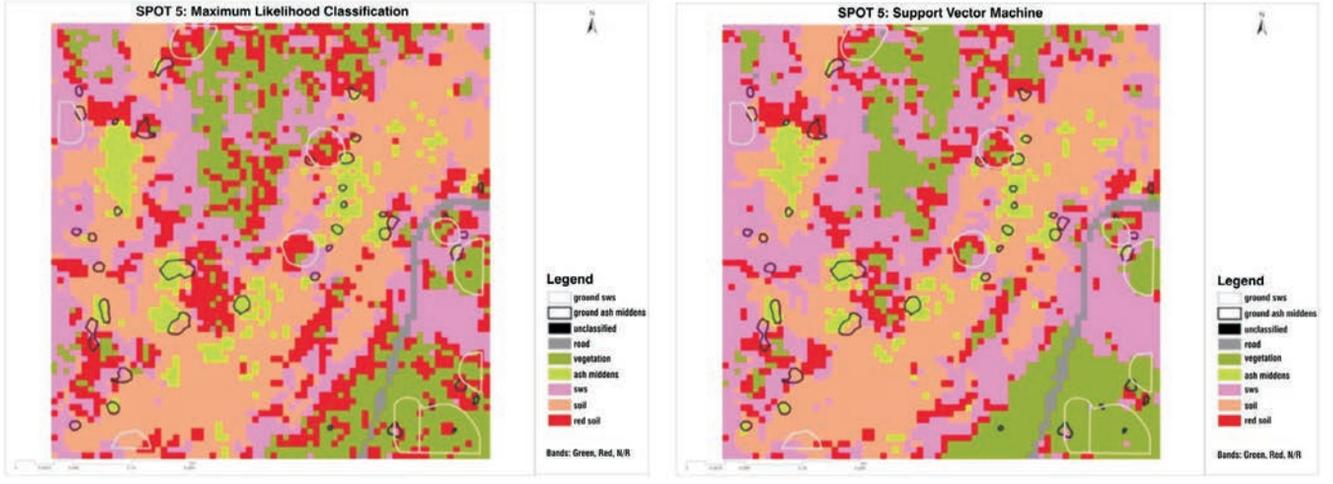


FIG. 6. (**Left**) *BC2 for SPOT5 classified using MLC.* (**Right**) *BC2 for SPOT5 classified using SVM.*

This content downloaded from
41.216.201.199 on Sat, 13 Jan 2024 10:54:34 +00:00
All use subject to https://about.jstor.org/terms

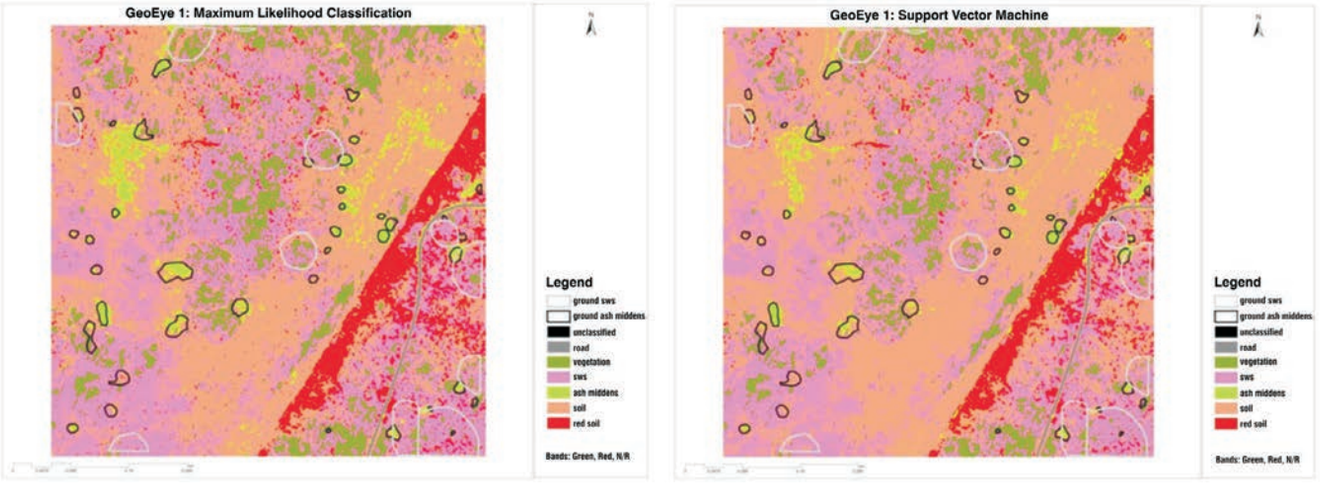


FIG. 7. (**Left**) *BC2 for GeoEye1 classified using MLC.* (**Right**) *BC2 for GeoEye1 classified using SVM.*

fied pixels was considered (i.e. accuracy assessment sites). Table 4 shows that both the user and producer accuracies are relatively high for ash middens. This corresponds with Figures 8–9 showing that the overall accuracy for ash middens is relatively high. The overall accuracy was higher on GeoEye1 compared to SPOT5. BC1 yielded very high results on GeoEye1 and SPOT5, but BC2 was not far behind on both images.

BAND COMBINATIONS

BC1 and BC2 did not perform vastly differently from the above-mentioned results when tested on the profiles. Figures 10 and 11 show the results of arbitrary profiles (pixels/band reflectance) on BC1 and BC2. GeoEye1 profiles are very narrow because of the greater number of pixels, while SPOT5 profiles are overly broad because of fewer pixels. There is a common

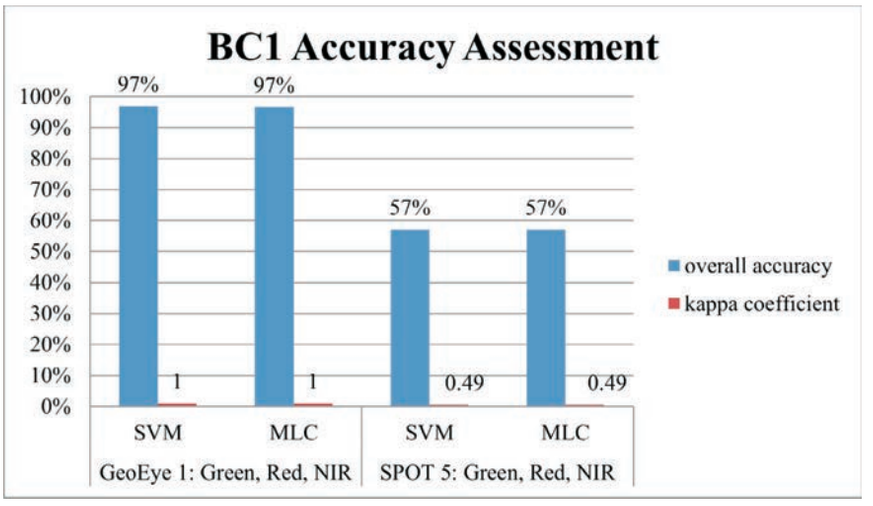


FIG. 8. *Accuracy assessment of the BC1 bands on SPOT5 and GeoEye1.*

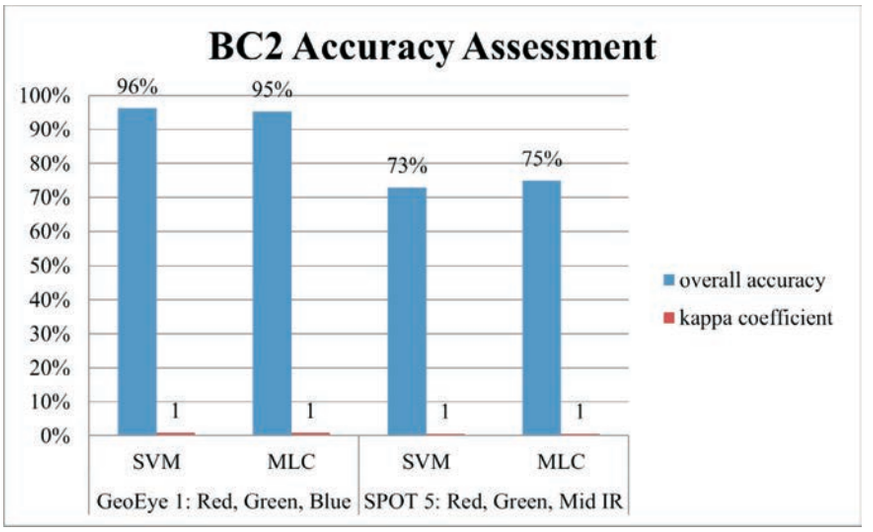


FIG. 9. *Accuracy assessment of the BC2 bands on SPOT5 and GeoEye1.*

This content downloaded from
41.216.201.199 on Sat, 13 Jan 2024 10:54:34 +00:00
All use subject to https://about.jstor.org/terms

TABLE 4. *Producer and user accuracies in percentage and pixels for MLC and SVM on GeoEye1 and SPOT5.*

Class	Producer accuracy Percentage	User accuracy Percentage	Producer accuracy Pixels	User accuracy Pixels
	SPOT5 MLC. Bands: green, red, near-infrared			
Ash middens	**93.55**	**87.88**	**29/31**	**29/33**
SWS	48.57	65.38	17/35	17/26
Soil	64.52	68.97	20/31	20/29
	SPOT5 SVM. Bands: green, red, near-infrared			
Ash middens	**90.32**	**93.33**	**28/31**	**28/30**
SWS	57.14	58.82	20/35	20/34
Soil	67.74	65.63	21/31	21/32
	GeoEye1 MLC. Bands: green, red, near-infrared			
Ash middens	**96.23**	**100**	**51/53**	**51/51**
SWS	90	93.75	45/50	45/48
Soil	100	98.15	53/53	53/54
	GeoEye1 SVM. Bands: green, red, near-infrared			
Ash middens	**100**	**100**	**53/53**	**53/53**
SWS	94	90.38	47/50	47/52
Soil	96.23	98.08	51/53	51/52
	GeoEye1 MLC. Bands: red, green, blue			
Ash middens	**96.23**	**98.08**	**51/53**	**51/52**
SWS	86	91.49	43/50	43/47
Red soil	100	98.15	53/53	53/54
	GeoEye1 SVM. Bands: red, green, blue			
Ash middens	**100**	**98.15**	**53/53**	**53/54**
SWS	88	93.62	44/50	44/47
Red soil	96.23	98.08	51/53	51/52
	SPOT5 MLC. Bands: red, green, mid-infrared			
Ash middens	**90.32**	**90.32**	**28/31**	**28/31**
SWS	68.57	64.86	24/35	24/37
Red soil	12.9	44.44	4/31	04/09
	SPOT5 SVM. Bands: red, green, mid-infrared			
Ash middens	**87.1**	**93.1**	**27/31**	**27/29**
SWS	57.14	68.97	20/35	20/29
Red soil	32.26	45.45	10/31	10/22

pattern of peaks on areas covered by ash middens from the profiles as can be seen on the relatively higher reflectance of ash middens on BC1 on both images. Figure 10 exhibits that the pixels of the three bands (appearing in different colours) have three distinct peaks that represent ash middens. It is worth noting that as expected, where the profile cuts across green vegetation, near-infrared is higher than where the profile cuts across soil.

DISCUSSION

ACCURACY ASSESSMENT AND KAPPA COEFFICIENT

In Figure 8, showing the accuracy assessment with BC1, the classification accuracy was higher on GeoEye1 (97% from MLC and SVM) compared to SPOT5 (57% from MLC and SVM). With BC2 (Fig. 9), a higher classification accuracy was again obtained on GeoEye1 compared to SPOT5. Nevertheless, MLC and SVM performed better on SPOT5 using BC2 (MLC: 75% and SVM: 73%). This means that the performance of these images is influenced by their respective bands. The addition of mid-infrared to green and red bands on SPOT5 improved the accuracy of MLC and SVM in classifying the land-cover classes. Replacing near-infrared with the blue band on GeoEye1 slightly decreased the accuracy. Mid-infrared and near-infrared are therefore the optimal bands for classifying the land-cover classes.

The kappa coefficient values further confirmed the accuracy assessment preliminary conclusions. A perfect relationship was achieved on GeoEye1 with BC1 and BC2. Therefore, the two band combinations are ideal for classifying ash middens and SWS. This is reasonable since the accuracy produced using BC1 and BC2 was very high (above 90%). However, SPOT5 presented a different scenario. A perfect relationship was achieved when using BC2, but not when using BC1. In this case, near-infrared is not an optimal band in classifying the five land-cover classes because its presence means that there is a poor relationship between ground-truthed pixels and the classification. Consequently, mid-infrared can be deemed an optimal band for SPOT5 based on its perfect relationship. Given the differences between BC1 and BC2 accuracy assessments, it is most likely that the features in the study area react similarly to near-infrared.

The detection of the ash middens and SWS is influenced by the properties of satellite imagery. The high classification accuracy on GeoEye1 can be attributed to its higher spatial (1.65 cm) and spectral resolution. There is enough detail on GeoEye1 to achieve the correct classification (and a high probability of classification and ground-truthed pixels, which is indicative of a perfect relationship). On the contrary, SPOT5's lower spatial resolution (10 m) gave rise to relatively low classification accuracy since the pixels cover larger areas (as mentioned earlier). This resulted in difficulties when assigning a region of interest to the correct land-cover class. Moreover, the lower spatial resolution may also mean that middens smaller than 10 m in extent may be easily missed when using this imagery.

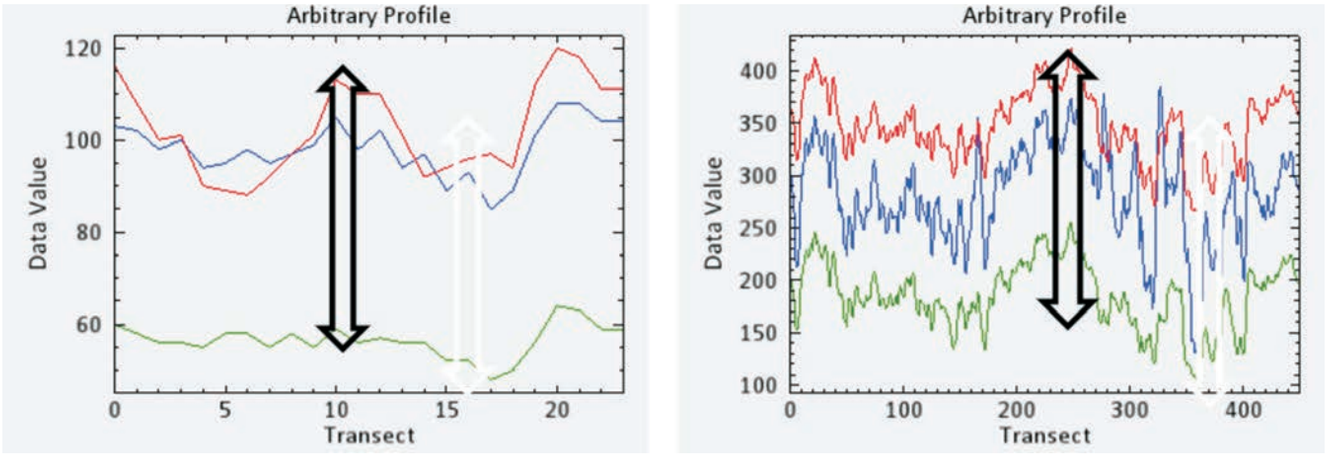


FIG. 10. *BC1 profiles.* (**Left**) *SPOT5.* (**Right**) *GeoEye1.*

This content downloaded from
41.216.201.199 on Sat, 13 Jan 2024 10:54:34 +00:00
All use subject to https://about.jstor.org/terms

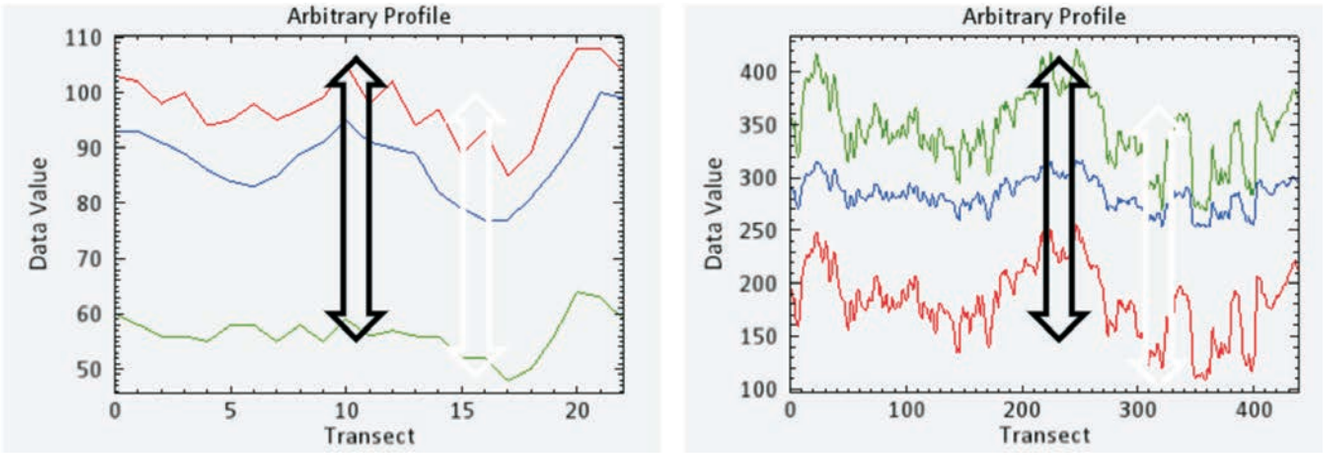


FIG. 11. *BC2 profiles.* (**Left**) *SPOT5.* (**Right**) *GeoEye1*.

The supervised classification techniques gave somewhat unexpected results. The expectation was that SVM, an advanced technique, would perform better than MLC on SPOT5 and GeoEye1. This expectation is founded on the performance of SVM on other images. For instance, SVM had higher classification accuracies when used for land-cover classification on Landsat (Rimal *et al*. 2019) and Sentinel-2 data (Mushtaq *et al*. 2021). However, MLC produced slightly higher accuracy (75%) on SPOT5 with BC2 than when using SVM (73%). The same can be seen from GeoEye1 where SVM accuracy results (96%) were higher by only 1% compared to MLC (95%). MLC and SVM classification techniques had the same accuracy (97%) when classifying using BC1. The classification techniques performed poorly when classifying with BC1 on SPOT5. Overall, SVM and MLC are good classification techniques on GeoEye1, irrespective of the band combination, and on SPOT5 provided that BC2 is used. However, MLC is a better classification technique than SVM on SPOT5 given the use of BC2. The spectral bands are responsible for higher classification accuracy of MLC, as mid-infrared increases the accuracy of MLC on SPOT5. Furthermore, the features in the study area may play a role, since Rimal *et al*. (2019) note that MLC can also show some higher accuracies due to the disparate signatures of open fields, while the disparate signatures of built-up areas resulted in higher SVM accuracy.

USER AND PRODUCER ACCURACY

Computing the accuracy assessment showed that some classes were better classified than others. The user and producer accuracies of the five land-cover classes were above 90% on GeoEye1 when using BC1 (only SWS, middens and soil accuracies are shown in Table 4 due to space). The results showed that there is a high probability that the pixels assigned as ash middens on the image were real ash middens on the ground. The use of BC1 did not yield the same results on SPOT5 as some of the classes such as soil and SWS were below 70%, but ash middens remained high at 93%. These slightly lower accuracy values indicate a misclassification of pixels, meaning that some areas on the ground classified as soil are not actually soil, for example. On average, using BC2 on GeoEye1 yielded high accuracies, nothing less than 80%, almost as high as when using BC1. Adding mid-infrared on SPOT5 saw ash midden accuracies remain high but soil decreased below 50% and SWS around 65% on average. Importantly, the addition of the blue band on GeoEye1 did not have a significant impact on the user and producer accuracies. Mid-infrared on SPOT5 increased the percentage of SWS but dropped that of soil compared to near-infrared. According to the high user and producer accuracies, ash middens were classified more accurately irrespective of the band combination or imagery, as opposed to soil.

BANDS AND SPECTRAL PROFILES

The spectral signatures of the bands led to the high reflectance of ash middens. The profile graphs on SPOT5 with BC1 show that there is a higher reflectance than on SPOT5 with BC2. The mid-infrared band reduced the level of reflectance meaning ash middens absorb relatively more light and heat on this band on SPOT5. Similar observations were made from GeoEye1 profiles. There is a slightly higher reflectance on GeoEye1 when using BC1 compared to BC2. The blue band reduces the level of reflectance on GeoEye1, meaning ash middens absorb relatively more light and heat on this band on GeoEye1. Consequently, ash middens can be clearly detected with multispectral satellite imagery because they have a higher reflectance, based on the image pixels, than the other classes (hence the peaks on the profile graphs). The overall high reflectance could be an indication of ash middens having a distinct spectral signature and that they reflect more radiance than they absorb. Ultimately, ash middens were best detected on SPOT5 with BC2 and on GeoEye1 with BC1 and BC2. This means high spectral resolution imagery is ideal for analysing ash middens regardless of the band combination. However, in the case of medium spectral resolution, one must select an optimal band combination for detecting ash middens, which is red, green, mid-infrared.

LIMITATIONS

One of the major limitations of this study is the low differentiation of the landscape, which makes it impossible to increase the land-cover classes. Moreover, ash that has mixed with background soil may cause confusion during the classification process, thereby resulting in misclassification. However, the spectral signature of the centre of each ash midden is invariably different from that of background soil. Further research using similar techniques may corroborate these results and show how far afield they are applicable.

CONCLUSION

Using remote sensing techniques to detect ash middens demonstrates a key step towards saving time and money when studying these, and potentially other, archaeological features. The high reflectance of ash middens relative to other land-cover classes has indicated that they have distinct spectral signatures. Overall, Band Combination 1 makes GeoEye1 the best

This content downloaded from
41.216.201.199 on Sat, 13 Jan 2024 10:54:34 +00:00
All use subject to https://about.jstor.org/terms

imagery but not very far ahead from using Band Combination 2. For SPOT5, replacing near-infrared with mid-infrared has noticeable implications hence using BC2 makes SPOT5 the optimal imagery for the detection of ash middens. One can say with confidence that the pixels assigned as ash middens on the image were really ash middens on the ground given the high user, producer and overall accuracy assessment results.

Certain bands perform better in classifying certain land-cover classes. Having near-infrared on SPOT5 lowered the producer and accuracy results of SWS and increased those of soil, while replacing it with mid-infrared increased SWS and decreased soil. Ash middens are well detected at medium resolution (SPOT5) ideally using BC2 but are best detected at high multispectral resolution (GeoEye1) with both BC1 and BC2. GeoEye1 is better than SPOT5 in the detection and analysis of ash middens because its high spectral and spatial resolution allows for more accurate mapping of ash middens. Support Vector Machine, although advanced, is not a significantly better supervised classification technique for classifying ash middens compared to Maximum Likelihood Classification. The techniques used in this study can be applied elsewhere in southern Africa for comparison considering the material making up the ash middens.

ACKNOWLEDGEMENTS

I thank Karim Sadr and Stefania Merlo for their contribution and feedback on the original MSc dissertation, which is the basis of this article.

REFERENCES

Abrams, M.J. & Comer, D.C. 2013. Multispectral and hyperspectral technology and archaeological applications. In: Comer, D.C. & Harrower, M.J. (eds) *Mapping Archaeological Landscapes from Space*: 57–110. New York: Springer.

Adelabu, S., Mutanga, O. & Adam, E. 2014. Evaluating the impact of red-edge band from Rapideye image for classifying insect defoliation levels. *Journal of Photogrammetry and Remote Sensing* 95: 34–41.

Aguirre-Gutierrez, J., Seijmonsbergen, A.C. & Duirenvoorden, J.F. 2012. Optimizing land cover classification accuracy for change detection, a combined pixel-based and object-based approach in a mountainous area in Mexico. *Applied Geography* 34: 29–37.

Astrium. 2013. SPOT: Accuracy and Coverage combined.

Boeyens, J.C.A. & Hall, S. 2009. Tlokwa oral traditions and the interface between history and archaeology at Marothodi. *South African Historical Journal* 61: 457–481.

Boeyens, J.C.A. & Plug, I. 2011. A chief is like an ash-heap on which is gathered all the refuse: the faunal remains from the central court midden at Kaditshwene. *Annals of the Ditsong National Museum of Natural History* 1: 1–22.

Bossard, M., Feranec, J. & Otahel, J. 2000. *CORINE Land Cover Technical Guide – Addendum 2000*. Technical Report No. 40. Copenhagen: European Environment Agency.

Comber, A.J. 2013. Geographically weighted methods for estimating local surfaces of overall, user and producer accuracies. *Remote Sensing Letters* 4: 373–380.

Comber A.J., Fisher, P., Brunsdon, C. & Khmag, A. 2012. Spatial analysis of remote sensing image classification accuracy. *Remote Sensing of Environment* 127: 237–246.

Denbow, J.R. 1979. *Cenchrus ciliaris*: an ecological indicator of Iron Age middens using aerial photography in eastern Botswana. *South African Journal of Science* 75: 405–408.

Digital Globe. 2014. GeoEye1.

ENVI. 2006. Environment for Visualising Images. Boulder, CO, USA: ITT Industries Inc.

Erener, A. 2013. Classification method, spectral diversity, band combination and accuracy assessment evaluation for urban feature detection. *International Journal of Applied Earth Observation and Geoinformation* 21: 397–408.

Keay, S.J., Parcak, S.H. & Strutt, K.D. 2014. High resolution space and ground-based remote sensing and implications for landscape archaeology: the case from Portus, Italy. *Journal of Archaeological Science* 52: 277–292.

Lasaponara, R. & Masini, N. 2011. Satellite remote sensing in archaeology: past, present and future perspectives. *Journal of Archaeological Science* 38: 1995–2002.

MacQuilkan, P. & Sadr, K. 2010. Remote sensing of archaeological ruins: a comparison. *Position IT* Nov/Dec: 50–51.

Maggs, T. 1976. Iron Age patterns and Sotho history on the southern Highveld: South Africa. *World Archaeology* 7: 318–332.

Mason, R.J. 1974. Background to the Transvaal Iron Age – new discoveries at Olifantspoort and Broederstroom. *Journal of the South African Institute of Mining and Metallurgy* 74: 211–216.

Mason, R.J. 1986. *Origins of Black People of Johannesburg and the Southern Western Central Transvaal AD350–1880*. Occasional Paper 16. Johannesburg: University of the Witwatersrand Archaeological Research Unit.

Mountrakis, G., Im, J. & Ogole, C. 2011. Support vector machines in remote sensing: a review. *ISPRS Journal of Photogrammetry and Remote Sensing* 66(3): 247–259.

Mushtaq, F., Mahmood, K., Chaudhry, M.H. & Tufail, R. 2021. A comparative study of support vector machine and maximum likelihood classification to extract land cover of Lahore District, Pakistan. *Pakistan Journal of Scientific and Industrial Research Series A*: *Physical Sciences* 64(3): 265–274.

Otukei, J.R. & Blaschke, T. 2010. Land cover change assessment using decision trees, support vector machines and maximum likelihood classification algorithms. *International Journal of Applied Earth Observation and Geoinformation* 12: 27–31.

Parcak, S.H. 2009. *Satellite Remote Sensing for Archaeology*. London and New York: Routledge.

Renfrew, C. & Bahn, P. 1991. *Archaeology: Theories*, *Methods and Practice*. London: Thames & Hudson.

Rimal, B., Rijal, S. & Kunwar, R. 2019. Comparing support vector machine and maximum likelihood classifiers for mapping of urbanization. *Journal of Indian Society of Remote Sensing* 48: 71–79.

Sadr, K. 2012. The origins and spread of dry laid, stone-walled architecture in pre-colonial southern Africa. *Journal of Southern African Studies* 38: 257–263.

Sadr, K. & Rodier, X. 2012. Google Earth, GIS and stone-walled structures in southern Gauteng, South Africa. *Journal of Archaeological Science* 39: 1034–1042.

Seddon, J.D. 1968. An aerial survey of settlement and living patterns in the Transvaal Iron Age: preliminary report. *African Studies* 27: 189–194.

Sisodia, P.S., Tiwari, V. & Kumar, A. 2014. A comparative analysis of remote sensing classification techniques. *2014 International Conference on Advances in Computing*, *Communications and Informatics (ICACCI)*: 1418–1421.

Siteleki, M.J. 2016. Detecting ash middens using remote sensing techniques: a comparative study in southern Gauteng, South Africa. Unpublished MSc dissertation. Johannesburg: University of the Witwatersrand.

Taylor, M. 1979. Late Iron Age settlements on the northern edge of the Vrededort Dome. Unpublished MA dissertation. Johannesburg: University of the Witwatersrand.

Tehrany, M.S., Pradhan, B. & Jebuv, M.N. 2014. A comparative assessment between object and pixel-based classification approaches for land use/land cover mapping using SPOT5 imagery. *Geocarto International* 29(4): 351–369.

Web References

http://www.satimagingcorp.com/ (accessed 6 April 2015).
http://www.sites.google.com/ (accessed 6 May 2015).
http://www.spotimage.com/ (accessed 13 May 2015).
http://www.harrisgeospatial.com/ (accessed 6 April 2015).
http://www.seos-project.eu/modules/remotesensing/remotesensing-c03- (accessed 13 May 2015).

This content downloaded from
41.216.201.199 on Sat, 13 Jan 2024 10:54:34 +00:00
All use subject to https://about.jstor.org/terms